CONF-781022--35

ENS/ANS INTERNATIONAL TOPICAL MEETING ON

NUCLEAR POWER REACTOR SAFETY

October 16-19, 1978 Brussels, Belgium

# RESULTS OF THE FIRST NUCLEAR BLOWDOWN TEST ON SINGLE FUEL RODS (LOC-11 SERIES IN PBF)



Jay R. Larson
Dennis R. Evans
Richard K. McCardell

EG&G Idaho, Inc.
P.O. Box 1625
Idaho Falls, Idaho 83401
United States of America

950 7781

# RESULTS OF THE FIRST NUCLEAR BLOWDOWN TEST ON SINGLE FUEL RODS (LOC-11 SERIES IN PBF)

Jay R. Larson
Dennis R. Evans
Richard K. McCardell

EG&G Idaho, Inc.
Idaho Falls, Idaho U.S.A.

## I. INTRODUCTION

This paper presents results of the first nuclear blowdown tests (LOC-11A, LOC-11B, LOC-11C) ever conducted. The Loss-of-Coolant Accident (LOCA) Test Series is being conducted in the Power Burst Facility (PBF) reactor at the Idaho National Engineering Laboratory, near Idaho Falls, Idaho, for the Nuclear Regulatory Commission. The objective of the LOC-11 tests was to obtain data on the behavior of pressurized and unpressurized rods when exposed to a blowdown similar to that expected in a pressurized water reactor (PWR) during a hypothesized double-ended cold-leg break. The data are being used for the development and verification of analytical models that are used to predict coolant and fuel rod pressure during a LOCA in a PWR.

## II. TEST DESCRIPTION, CONDUCT, AND RESULTS

The tests were conducted with four, separately shrouded, PWR-type fresh fuel rods. The fuel rods were of 15 x 15 design, except for the active length, which was 0.91 m. The plenum volume was scaled proportionally to the active fuel length. Two rods were initially pressurized to 0.1 MPa (Rods 611-1, 611-4) and one each to 2.11 MPa (Rod 611-3) and 4.82 MPa (Rod 611-2). (However, the 4.82-MPa rod contained a small leak and its posttest pressure was 1.0 MPa.) A fluted flow shroud was selected to minimize the chance of complete flow blockage if uniform ballooning occurred. The coolant flow area was about twice the value associated with a single PWR rod. Four screws, located at two axial elevations, centered each fuel rod. Figure 1 illustrates the blowdown system and a test fuel rod within a fluted shroud.

Valves were used to isolate the experimental hardware from the PBF loop coolant system and thereby provide a controllable flow path during blowdown. Test conduct began with PBF loop isolation from the in-pile tube and a simultaneous reactor scram. Blowdown

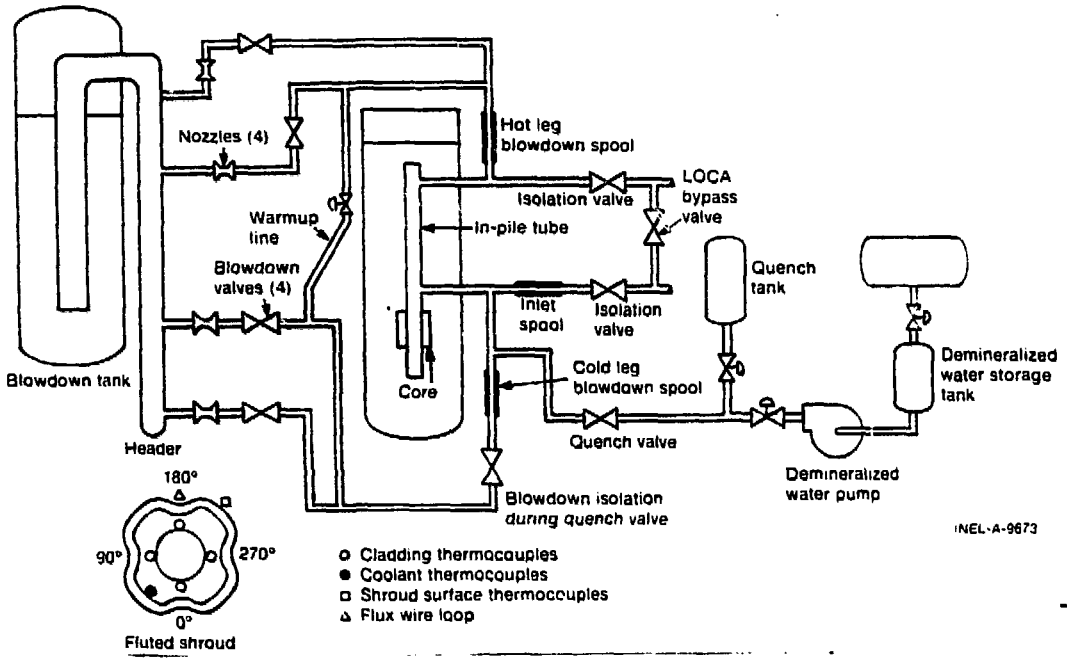


Fig. 1 PBF blowdown system and Test LOC-11 fuel rod orientation.

then commenced and was controlled by quick (~ 100 ms) opening blowdown valves. Valve operation was controlled by a time sequential programmer. The break planes were formed by converging-diverging nozzles with a cylindrical throat section having equal length and diameter measurements. The design was patterned after that used in the Semiscale program at the Idaho National Engineering Laboratory to optimize predictive capability. The throats were sized to control the flow and depressurization rates. The coolant ejected from the system and the fission products carried from the fuel were collected in a blowdown tank. A quench system provided coolant for terminating the cladding temperature excursion and ending the test.

The fuel rod instrumentation consisted of cladding surface thermocouples, fuel centerline thermocouples, linear variable differential transformers, plenum pressure transducers, and plenum temperature thermocouples. The test train instrumentation consisted of flow turbines located at each end of the fuel rod flow shrouds, coolant temperature thermocouples, coolant pressure transducers, and thermocouples on the outer surface of the fuel rod flow shroud.

Piping measurement spools were installed for determination of the initial inlet and blowdown coolant conditions. Each spool contained temperature, pressure, and flow rate measuring devices. The spools in the blowdown piping also contained a shielded and chopped three-beam gamma densitometer to determine coolant density, and inlet screens to straighten and disperse the flow. This first application of a gamma densitometer in a reactor radiation field was successful even though the field changed from near 2000 R/h to a small value in 30 seconds.

The LOC-11 tests consisted of three separate blowdowns from nuclear power operation. The first test (Test LOC-11A) was conducted after a power calibration, two cycles of full power operation for preconditioning, and an additional six hours at full power. Initial test conditions were a coolant inlet pressure of 14.9 MPa, temperature of 591 K, flow rate of 0.91 ℓ/s, and a peak power of 39.1 kW/m. Spurious system blowdown and isolation valve cycling occurred because of an inductive feedback from a liquid level indicator in the blowdown tank interrupting the electrical signals required to activate proper valve sequencing. As a result, additional coolant entered the blowdown system from the PBF loop, thus delaying the onset of critical heat flux (CHF) for six to eight seconds after blowdown initiation. Peak measured cladding temperatures did not exceed 830 K. Test LOC-11A served as a facility checkout test and is not considered further.

Tests LOC-11B and LOC-11C were conducted with axial peak powers of 45.5 and 69.9 kW/m, inlet coolant pressures of 15.2 and 15.3 MPa, inlet coolant temperatures of 593 and 596 K, and flow rates per rod of 0.99 and 0.98 ℓ/s, respectively. During Test LOC-11B, blowdown system isolation and reactor scram occurred at time zero, with one blowdown valve opening in the hot- and cold-leg piping at about 0.9 second, as planned. The delay in valve opening allowed for a 0.9-second stagnation period prior to blowdown. Blowdown was programmed to begin about 0.1 second after isolation and reactor scram during Test LOC-11C, rather than the 0.9-second delay used for Test LOC-11B. CHF occurred 3.2 seconds after isolation during Test LOC-11B, and peak measured cladding temperatures reached 880 K. During Test LOC-11C, CHF occurred 1.6 seconds after isolation, and the peak measured cladding temperatures reached 1030 K.

To aid in understanding the test results, and to evaluate prediction capability, the RELAP4/MOD6[1][a] computer code was used for posttest calculations of the coolant behavior and the FRAP-T[2][b] code was used to calculate the fuel rod behavior.

Figure 2 compares the Test LOC-11C posttest calculations and measured coolant pressure at the inlet spool. During blowdown the coolant pressure throughout the system is essentially uniform, with the pressure drop to the blowdown tank occurring at the break planes. From the initial steady state value the pressure drops sharply when the blowdown valves open (subcooled decompression). The saturated depressurization is slightly over-predicted to two seconds and underpredicted beyond ten seconds. These slight differences may be attributed to small errors in the calculation of stagnation conditions used to evaluate break flow rates.

Figure 3 compares the calculated and measured mass flow rate in the hot-leg spool. The measurement was obtained by averaging values obtained by combining independent measurements of volumetric flow rate, momentum flux, and density, two-at-a-time,

[a] RELAP4/MOD6, Update 4, EG&G Idaho, Inc. Configuration Control Number H00332IB.

[b] FRAP-T4, MOD4, Version 03/21, EG&G Idaho, Inc., Configuration Control Number H00286IB.

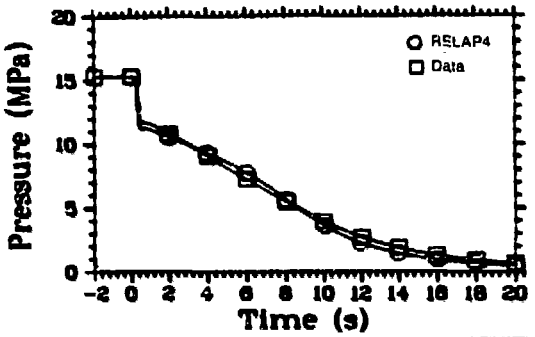

Fig. 2 Pressure at the inlet spool.

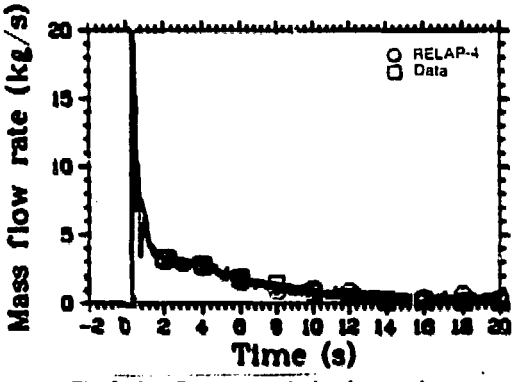

Fig. 3 Mass flow rate at the hot-leg spool.

assuming homogeneous flow. The chordal densities from the three-beam gamma densitometer indicated that the measurement spool screen did not completely disperse the liquid and vapor phases. However, an average piping cross section density was determined by integrating an assumed linear gradient fitted to the chordal densities. On the basis of these assumptions, the measured mass flow rate and the calculation are in good agreement.

Figure 4 compares the calculated and measured volumetric flow measurements at the lower end of Rod 611-1. The reverse flow spike and the slight positive flow during the initial six seconds generally compare well with the calculations. However, the initial reverse flow is calculated to decrease to near zero somewhat earlier than measured. This forces the code calculations into CHF somewhat earlier than measured. Beyond six seconds, RELAP4 underpredicts the flow and then predicts more reverse flow than occurs.

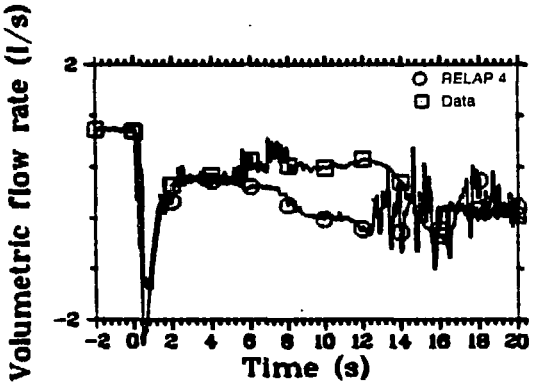

Fig. 4 Volumetric flow rate at Rod 611-1 inlet.

The reverse flow spike results from the higher initial enthalpy in the upper plenum maintaining a higher saturation pressure in the upper plenum than in the lower plenum. As the plenum pressures equalize, a 20% larger flow resistance through the cold-leg flow path than through the hot-leg flow path likely causes coolant to flow upward through the fuel rod shroud. After 15 seconds, the flow direction reverses because the lower plenum-downcomer volume becomes depleted of mass sooner than the larger upper plenum-bypass volume. The upper plenum then depressurizes more slowly than the lower plenum, thus causing the flow reversal.

Calculation of the fuel rod shroud volumetric flow rate and direction is difficult for several reasons. The calculated transient shroud pressure drops are a few hundredths of an MPa, which means small errors in the calculated plenum pressures result in large errors in

shroud flow rate. Phase separation in the plena and countercurrent flow in the shrouds are suspected, but are not treated exactly by the empirical models in the code. An unplanned bypass leakage path in parallel with the shrouds was discovered during pretest operation. The magnitude (30 to 35% of total shroud flow rate) was variable and its location was not resolved by limited posttest checks.

Also, with increasing time the density decreases significantly, meaning apparent errors in volumetric flow rate are really only small errors in mass flow rate.

Figure 5 shows the calculated and measured cladding surface temperatures on Rod 611-1. The calculated temperature includes the effect of thermal radiation to the relatively cold shroud, which becomes important at high coolant quality. Without radiation the calculated temperature would continue to increase after about 10 seconds, reaching a maximum at 30 seconds. CHF is calculated to occur when the fuel rod flow rate returns to a low value at about 1.1 seconds. The measured peak cladding temperature (at about 15 seconds) is about 100 K less than predicted. Likely causes of the discrepancy are differences in calculated and actual post-CHF heat transfer and differences in calculated and measured time to CHF.

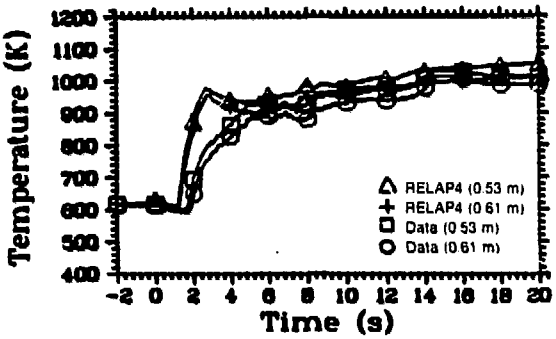

Fig. 5 Cladding surface temperatures for Rod 611-1.

The RELAP4 calculations, using a low flow pool boiling CHF correlation (modified Zuber), indicated that CHF would not occur during the initial flow stagnation period, but would occur when the initial negative flow spike returned to near zero. Tests LOC-11B and LOC-11C results confirmed that CHF did occur after the stagnation period when the shroud flow rate reached near zero at 3.1 and 1.6 seconds, respectively.

Figure 6 compares measured cladding temperature, shroud inlet and exit volumetric flow rate, and cladding elongation for Rod 611-3. CHF occurs when the flow rate within the shroud is zero. The elongation sensor also indicates CHF at essentially the same time as the thermocouple, implying that CHF likely occurred simultaneously over the central portion of the rod, including the area of the lower thermocouple.

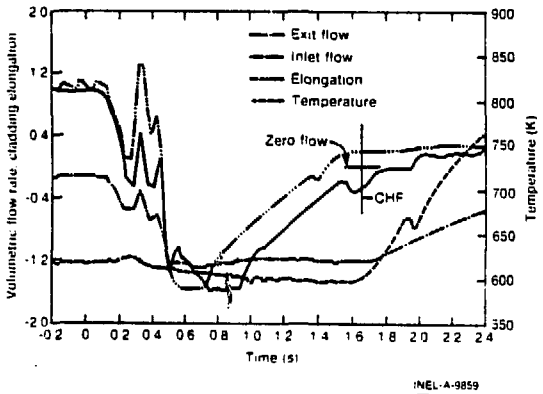

Fig. 6 Comparison of shroud volumetric flow rate, cladding elongation, and cladding surface temperature during LOC-11C.

Figures 7 and 8 compare FRAP-T calculations with data for the cladding

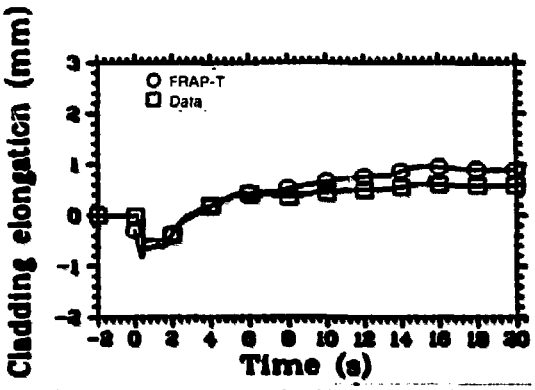


Fig. 7 Cladding elongation during blowdown for Rod 611-1.

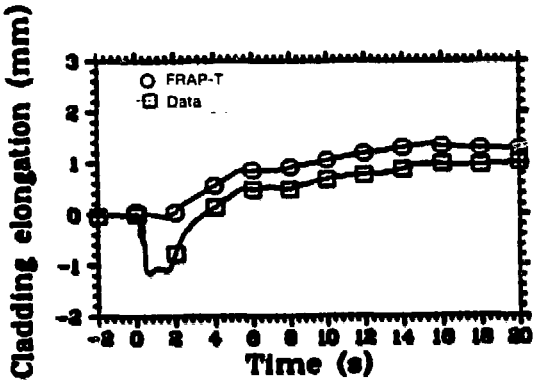


Fig. 8 Cladding elongation during blowdown for Rod 611-3.

elongation during blowdown for Rods 611-1 and 611-3. The data and calculations have been normalized to show only the relative change during the transient. The data indicate trends in behavior but not absolute values[a]. With scram, the elongation sensor indicates a significant shortening of the rod, believed to be caused by a contraction in the fuel length corresponding with the sharp drop in fuel temperature, and release of elastic strains in the cladding caused by contact with the fuel stack during the initial rise in power. After the shrinkage, the elongation remains constant until the onset of CHF. With CHF, the elongation increases because of thermal expansion of the cladding corresponding to the cladding temperature.

The sharp drop in elongation calculated for the relatively unpressurized rod occurs because of contact between the fuel pellets and the cladding during the initial power increase. At about 0.6 second the gap begins to open, relaxing the elastic strains caused by interaction. The axial differential pressure force causes a slight length increase. Further elongation is caused only by thermal expansion. The calculation for the pressurized rod does show a shrinkage, but the elongation returns to its initial value almost instantaneously as the gap opens. The lack of agreement during the transient is not surprising since the calculation would likely fail to predict the correct fuel-cladding contact during steady state operation. Further, calculated elongation is caused only by thermal expansion as the cladding temperatures rise, peak, and decline.

Upon test trains dissassembly the rods were found to be covered with a dark-grey oxide and a thin layer of crud. Posttest diametral profiles for the test fuel rods are illustrated in Figure 9. The cladding of the unpressurized rods, Rods 611-1 and 611-4, was slightly collapsed (about 0.1 mm) over a centrally located axial span of 0.4 m. The cladding of the pressurized rods was slightly ballooned over a centrally located span of 0.18 m, with the maximum swelling of 1.4 and 2.5% for the intermediate and high pressure rods, Rods 611-3 and 611-2, respectively, occurring near the axial peak power location. The

[a] Measurement device was not compensated for temperature change.

larger magnitude of ballooning for Rod 611-2 suggests that the internal pressure of the rod was higher than that for Rod 611-3 during Test LOC-11C. That is, the leak may have occurred during or after the ballooning process.

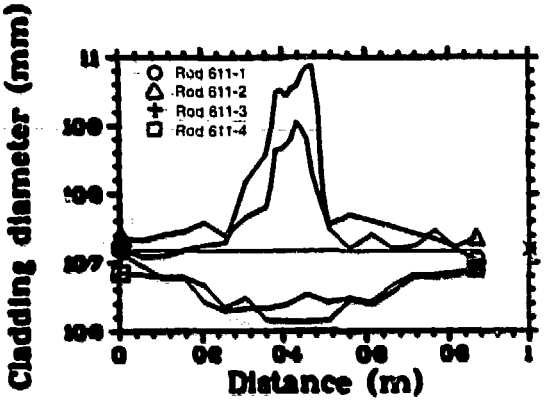

Fig. 9 Cladding diameter along the fuel stack.

Figure 10 compares the FRAP-T calculation for circumferential strain with the data from Rod 611-3. The maximum calculated cladding ballooning is overpredicted (calculated increase – 5.5%). The calculated axial location of the maximum corresponds with the axial power peak input to the code. A finer axial nodalization of the test rod would probably improve correspondence between the calculated and measured regions of the cladding ballooning. A comparison of the FRAP-T calculation of cladding deformation for the low pressure rods with the data from Rods 611-1 and 611-4 is shown in Figure 11.

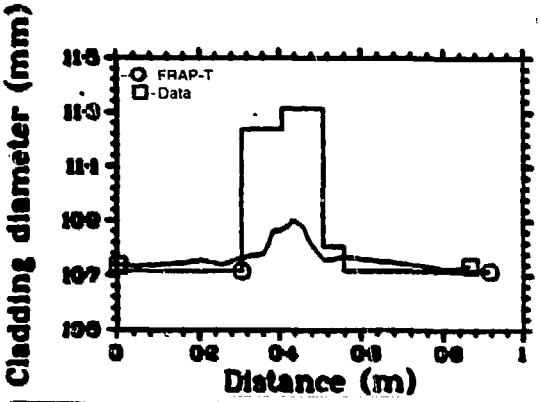

Fig. 10 Cladding diameter along the fuel stack for Rod 611-3.

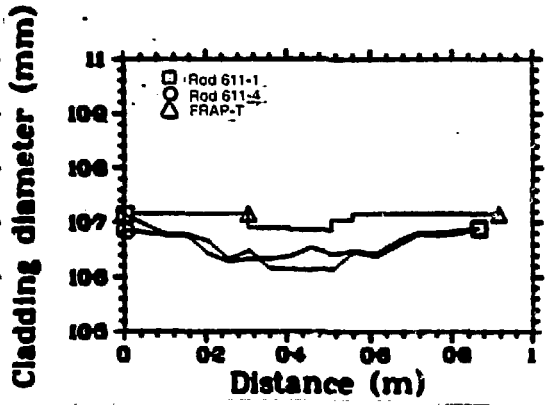

Fig. 11 Cladding diameter along fuel stack for Rods 611-1 and 611-4.

The calculated results indicate the FRAP-T model is overpredicting the internal pressure during blowdown. The FRAP-T calculations were performed using an approximation to the measured cladding temperature as a boundary condition, with an assumed axial temperature distribution based on RELAP4 calculations.

## III. CONCLUDING STATEMENT

The first PBF-LOCA program test, consisting of three sequential blowdowns from nuclear operation, was conducted with four, separately shrouded, fresh PWR-type fuel rods. Fuel rod cladding collapse and swelling occurred when the unpressurized and pressurized rods were exposed to the blowdown conditions and to measured cladding temperatures up

to 1030 K. Calculations of cladding deformation based on an approximate model overpredicted ballooning and underpredicted collapse. Calculated break flow rate was in good agreement with measurements. However, calculated flow rates in the fuel rod shrouds did not correspond as well to measurements because of modeling problems with an unplanned variable bypass leakage, phase separation and countercurrent flow, and small errors in pressure calculation. Calculated cladding surface temperatures were about 100 K higher than those determined using surface mounted thermocouples. Thermal radiation from the fuel rod was significant during the blowdown when the coolant quality was high.

## IV. REFERENCES


1. K. R. Katsma et al, *RELAP4/MOD5 – A Computer Program for Transient Thermal-Hydraulic Analysis of Nuclear Reactors and Related Systems, Volume I-III*, ANCR-NUREG-1335 (September 1976).

2. J. A. Dearien et al, *FRAP-T2 – A Computer Code for the Transient Analysis of Oxide Fuel Rods*, TREE-NUREG-1040 (April 1977).